Am J Transl Res 2019;11(9):5752-5763
www.ajtr.org /ISSN:1943-8141/AJTR0095771

Original Article

DHT deteriorates the progression of monocrotaline-induced pulmonary arterial hypertension: effects of endogenous and exogenous androgen

Juan Wen[1*], Jiajie Wang[2*], Xiaohong Tang[1], Shangbin Deng[3], Jia Dai[1], Xiaohui Li[4], Weijun Cai[2]

Departments of [1]Cardiology of The 3rd Xiangya Hospital, [2]Histology and Embryology, School of Basic Medicine, Central South University, Changsha, Hunan, China; [3]Department of Orthopaedics, 8th Hospital of Changsha, Changsha, Hunan, China; [4]Department of Pharmacology, Xiangya School of Pharmaceutical Sciences, Central South University, Changsha, Hunan, China. [*]Equal contributors.

Received April 11, 2019; Accepted August 8, 2019; Epub September 15, 2019; Published September 30, 2019

Abstract: Pulmonary arterial hypertension (PAH) is more popular among females than males. However, female patients exhibit better prognosis than men, sex hormones may partly explain such sex paradox. Estrogens are disease modifiers in PAH, androgen effects on PAH are yet incompletely characterized. In this study, we sought to determine the effect of androgen depletion and dihydrotestoterone (DHT) repletion on a rat model of monocrotaline-induced PAH (MCT-PH) and to further clarify the possible mechanisms. MCT-PH was induced in male Sprague-Dawley (SD) rats as well as castrated rats with or without concomitant DHT repletion. Our research showed that rats with PAH exhibited cardiopulmonary alterations including induction of right ventricular systolic pressure (RVSP), pulmonary vascular remodeling, right ventricular hypertrophy (RVH) and fibrosis. Moreover, MCT upregulated expression of vascular cell proliferative proteins (PCNA and Ki67), matrix metalloproteinase-2 (MMP-2) and apoptotic proteins (Bax and Bcl-2) in pulmonary artery, and promoted pro-inflammatory cytokines expression (IL-6, TNF-α and IL-1β) and oxidative stress level (SOD activity and MDA level) in perivascular lung tissue. The magnitude of these PAH-induced changes was significantly partly inhibited by castration. DHT replacement reversed castration-action on MCT-related cardiopulmonary alteration. We studied the detrimental effect of endogenous androgen and exogenous DHT in MCT-PH rats, which may be through stimulation of vascular cell proliferation, gelatinolytic activity, apoptosis, perivascular inflammation and oxidative stress.

Keywords: Androgen, dihydrotestoterone, pulmonary arterial hypertension, right ventricular hypertrophy, vascular remodeling

Introduction

PAH is a progressive disease characterized by a sustained increase in pulmonary arterial pressure driven by vascular remodeling. Eventually, this leads to subsequent RVH and heart failure [1, 2]. Gender difference was reported in the incidence, susceptibility and prognosis of PAH [3, 4]. Female susceptibility to PAH has been evidenced by recent epidemiological studies, and most recent figures show a female-to-male ratio of 4:1. This high incidence of women is almost present in all PAH subtypes [5, 6]. One hypothesis that may explain the female susceptibility in PAH is that female hormone estrogen is detrimental and androgen is protective in the setting of pulmonary hypertension. However, male PAH patients exhibit poorer survival than female patients [6-8], such sex paradox suggests a role of complex sex hormone signaling and processing pathways in PAH [9]. The role of estrogen and its metabolites on PAH have been well-established, but fewer studies focus on androgen action.

Testosterone (T) and DHT are two natural potent androgens in the mammalian system. Both T and DHT bind to the same androgen receptor (AR) in the cytoplasm of target cells, T can be converted to DHT by 5a-reductase, and DHT exerts higher affinity to AR and stronger androgenic activity than T [10]. T has been shown to

vasodilate isolated pulmonary arteries in rats and humans [11, 12]. DHEA, the precursor steroid hormone to T, can inhibits hypoxia-induced vasoconstriction of the pulmonary arteries (PA) [13, 14], as well as improves RV function [15]. However, in the cardiac setting T has been shown a detrimental effect on overall RV function in the context of increased afterload [16], the key role of androgen on modulating PA remodeling still lacks of evidence. In our previous studies, we demonstrated that DHT, which avoids the estrogen action of T participated in vascular angiogenesis [17], and we further explored whether endogenous androgen and exogenous DHT (5 mg/kg/d) repletion has regulatory effect on the progression of PAH.

MCT has been suggested to induce vascular remodeling, and develop PAH in rats with 3 weeks in previous study [18]. In the present study, we used this rat model of MCT-induced PAH to investigate the effect of endogenous and exogenous androgen on pathological changes such as vascular remodeling and RVH, and the potential mechanisms were also explored.

Material and methods

Ethics statement

This study was carried out in strict accordance with the recommendations in the Guide for the Care and Use of Laboratory Animals of the National Institutes of Health. The protocol was approved by the Animal Ethics Committee of the 3rd Xiangya Hospital of Central South University. All efforts were made to minimize suffering.

MCT-induced PAH model and experimental design

Sexually mature male SD rats weighed 200-250 g were supplied by the Beijing Vital River Laboratory Animal Technology Co Ltd. Rats were anesthetized with chloral hydrate anesthesia (3 ml/kg, i.p) and randomly receiving castration (n = 28) or sham castration (n = 28). To induce PAH, rats were received single intraperitoneal injections of MCT at 60 mg/kg after 1 week following surgery. Sham rats were divided into two groups:control group (n = 13) and MCT group (n = 15), castrated rats were also assigned into two groups: Cas + MCT group (n = 14) and Cas + MCT + DHT group (n = 14). Rats in control groups received single intraperitoneal injections of sterile PBS at volumes equivalent to the MCT dosing. Accordingly, all rats were dosed once daily with 0.1 mL of peanut oil or DHT (Sigma-Aldrich, 5 mg/kg dissolved in peanut oil) subcutaneously for 3 weeks. **Figure 1A** shows the experimental timeline. The dosage and duration of the treatment were based on protocols previously described [19]. On day 28, animals were anesthetized with sodium pentobarbital (30 mg/kg, i.p).

Hemodynamic analysis and ventricular weight measurement

After feeded with peanut oil or DHT for 4 weeks, rats were placed on a thermo-regulated surgical plate. The body weight was recorded and the RV catheterization was performed to monitor RVSP. The right and left ventricle (RV, LV) and the interventricular septum (S) were dissected after the animals were sacrificed. The ratio of RV/(LV + S) was calculated to evaluate the extent of RVH.

Tissue preparation

Lung, pulmonary artery and RV tissues were fixed in 4% paraformaldehyde overnight and then dehydrated with an alcohol gradient. Paraffined tissues were embedded in paraffin and cut to 5-μm sections. Cryosections were sliced into 4-μm thick sections and fixed in 4% paraformaldehyde and permeabilized in PBS/0.5% Triton, and then incubated in 0.2% BSA-C. Paraffined tissues were used for HE staining and Sirius red staining, cryosections were used for immunofluorescence.

Histological analysis

HE staining was performed on vessel sections for measurement of wall thickness (WT). The PA with a diameter of 50~150 μm was evaluated. The vessel outer diameter (ED) and internal diameter (ID) was measured to calculate WT (WT = (ED-ID)/ED). HE staining and Sirius red staining was also performed on RV to evaluate the cross-sectional area of cardiomyocytes and the degree of RV fibrosis, respectively. Images were analyzed using Image-Pro Plus 6.0 software and averaged by observers blinded to the experimental protocol. The values provided were the average of 10 fields of view for 10 sec-

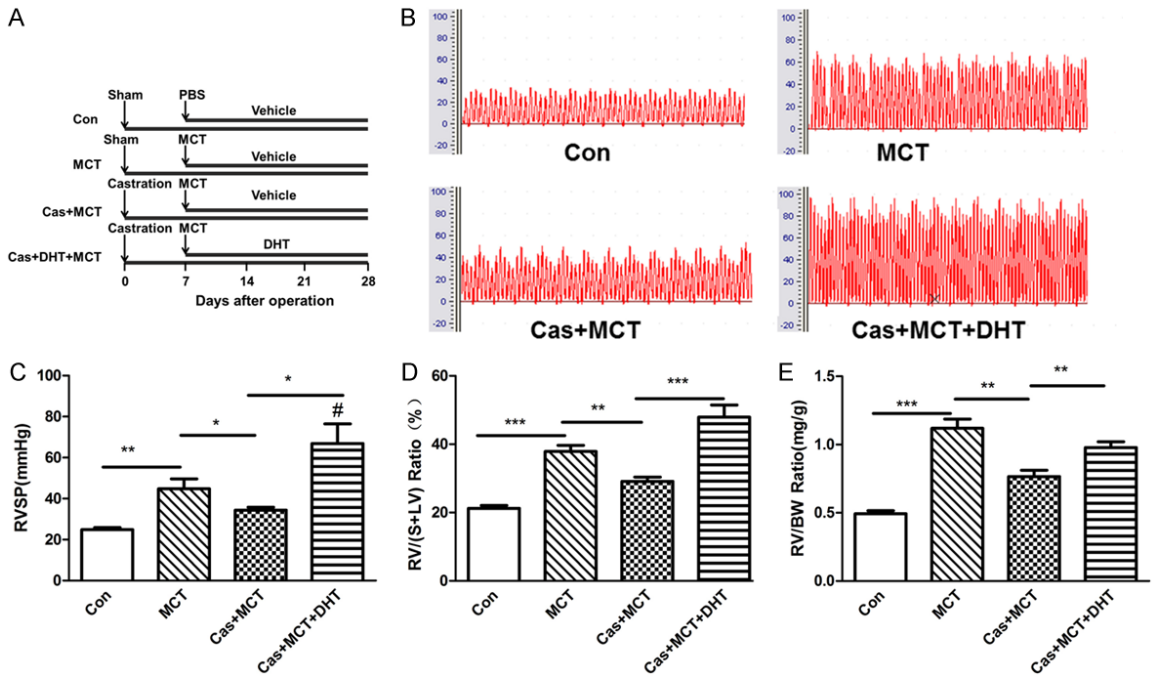

Figure 1. Effect of castration and/or DHT replacement on RVSP and RV mass in MCT-PH rats. Experimental design: A. Adult male SD rats were assigned to 4 groups as follows: Con group (sham castrated rats with injection of vehicle controls), MCT group (sham castrated rats were injected with MCT at a dose of 60 mg/kg to induce MCT-PH animal model), Cas + MCT group (castrated rats were injected with MCT) and Cas + MCT + DHT group (castrated rats with MCT-PH were injected with DHT daily for 3 weeks). B. Representative pictures of RVSP waves in each group by the right heart catheterization. C. Bar graphs were summary data for RVSP level. D, E. Result of RV mass assessed by RV/(LV + S) and RV/BW. *P<0.05, **P<0.01, ***P<0.001 between groups. $^{\#}$P<0.05 vs. the MCT group.

tions per rat, and the cross-sectional area of cardiomyocyte was determined on 60-80 transversely cut myocardial fibers from 5 to 6 rats in each group.

Oxidative stress factors

Isolated lung tissue was homogenized in pre-chilled PBS and centrifuged at 3000 g for 15 minutes at 4°C. The supernatant was collected and tested for MDA content and SOD activity by ELISA (Nanjing Institute of Bioengineering, China).

Real-time PCR

Total RNA was extracted from tissues using TRIzol (Invitrogen, USA). cDNA was synthesized using a Transcriptor First Strand cDNA Synthesis Kit (Thermo, USA). qRT-PCR experiments were performed using FastStart DNA Master SYBR Green I Kit (Bio-Rad, USA). Primer sets specific for ANP, BNP, TGF-β, TNF-α, IL-6 and IL-1β were listed as follows: The mouse atrial natriuretic peptide (ANP) primers were forward (5'-CAG CAC AAT AGA GCC GCT GA-3') and reverse (5'-GGG CAG GAG CTT GA A CAC G-3'), mouse brain natriuretic peptide (BNP) primer were forward (5'-GCA GAA GCT GCT GGA GCT GA-3') and reverse (5'-ATC CGG AAG GCG CTG TCT TG-3'), mouse TGF-β primer were forward (5'-ATT CCT GGC GTT ACC TTG G-3') and reverse (5'-TGT ATT CCG TCT CCT TTG GTT C), mouse TNF-α primer were forward (5'-GCA TGA TCC GAG ATG TGG AAC TGG-3') and reverse (5'-CGC CAC GAG CAG GAA TGA GAA G-3'), mouse IL-6 primer were forward (5'-AGG AGT GGC TAA GGA CCA AGA CC-3') and reverse (5'-TGC CGA GTA GAC CTC ATA GTG ACC-3'), mouse IL-1β primer were forward (5'-GCT GTC CAG ATG AGA GCA TC-3') and reverse (5'-GTC AGA CAG CAC GAG GCA TT-3'). GAPDH was used as an internal control. The relative mRNA expression levels were calculated by the $2^{-\Delta\Delta Ct}$ method.

Western blot analysis

Western blot analysis was performed as described previously [20]. Tissues were lysed

and homogenized in RIPA buffer. Equal amounts (40 ug) of proteins were fractionated on 10% or 12% SDS-PAGE, and transferred to a PVDF membrane (Millipore). The membrane was blocked with TBST buffer containing 5% skim milk powder for 2 hours at room temperature and incubated with antibodies against Bax (Proteintech, China, 1:1000), Bcl-2 (Proteintech, China, 1:1000), PCNA (SantaCruz, USA, 1:500), MMP-2 (Vector lab, UK, 1:1000) and β-actin (Proteintech, China, 1:1000) overnight at 4°C, respectively. After washed for 3 times, the membrane was incubated for 1 h at room temperature with horseradish peroxidase-conjugated secondary antibody (Proteintech, China, 1:5000). The signal was visualized using a Typhoon scanner after exposed to ECL detection reagent. β-actin was used as an internal control. The specific signals of target protein were quantified by the Image Lab software, and the data was presented as fold of vehicle control after normalizing protein input based on β-actin levels.

Immunofluorescence staining

Cryosections were incubated overnight at 4°C with primary antibodies against rabbit Ki67 (Vector lab, 1:400) and rabbit MMP-2 (Vector lab, 1:400). Biotin SP-conjugated AffiniPure donkey anti-rabbit IgG (Dianova GmbH, 1:300) secondary antibodies was followed by Cy3-conjugated streptavidin (Biotrend). The nuclei was stained with DAPI (Invitrogen in USA). The sections covers lipped and viewed with a Nikon confocal microscope, the fluorescence intensity analysis was performed using Nikon EZ-C1 3.90. The values provided were the average of 10 fields of view for 10 sections per rat.

Statistical analysis

All experiments were performed at least three times for each determination. Data are presented as the Mean ± SEM. Differences in measured variables between groups were determined by one-way ANOVA analysis of variance followed by the Student-Newman-Keul test for multiple comparisons. $P<0.05$ was considered statistically significant. Statistical analysis was performed with SPSS software version 13.0.

Results

Castration attenuates MCT-induced increases in RVSP and RVH, whereas DHT replacement worsens castration-mediated action

There was no difference in baseline body weight (BW) among four groups. One rat in MCT group and one rat in Cas + MCT group were dead. As shown in **Figure 1B** and **1C**, MCT-PH rats developed a significant elevation of RVSP compared to those in control group (50.81±5.37 mmHg vs. 24.92±0.92 mmHg; $P<0.05$), indicating that PAH model was built successfully. However, in MCT-PH group, castration decreased RVSP compared to sham castration (34.40±1.36 mmHg vs. 44.79 + 4.83±0.92 mmHg; $P<0.05$), and DHT reversed the decrease in RVSP produced by castration effectively ($P<0.05$). Interestingly, RVSP in Cas + MCT + DHT group was even higher than MCT group (66.85±9.63 mmHg vs. 44.79±4.83 mmHg; $P<0.05$). The ratio of RV/(LV + S) and RV/BW was calculated to evaluate the extent of RV mass (**Figure 1D** and **1E**). MCT increased ratio of RV/(LV + S) significantly compared with the control group ($P<0.01$), which was decreased by castration ($P<0.01$). Furthermore, this effect was reversed by DHT replacement notably ($P<0.001$, **Figure 1D**). Similarly, MCT led to an increase in RV/BW ratio compared to the control group ($P<0.001$, **Figure 1E**), and castration significantly reduced RV/BW ratio ($P<0.01$), which was also partly inhibited by DHT ($P<0.01$).

Castration improves pulmonary arterial remodeling, whereas DHT replacement dramatically worsens castration-induced effect

To understand the effect of androgen on pulmonary vascular remodeling, we evaluated the medial wall thickness in PA by HE staining. The result showed that MCT led to PA remodeling in comparison to the control group ($P< 0.001$). The smooth muscle cells were shown to be disordered and intimate hyperplasia, and the elastic fibers were distorted, which indicated that vascular remodeling had occurred (**Figure 2A-D**). The medial WT of PA in castrated rats with MCT-PH was significantly lower than that in sham-castrated rats with MCT-PH ($P<0.001$), while the DHT replacement could worsen the degree of vascular remodeling ($P<0.001$; **Figure 2E**).

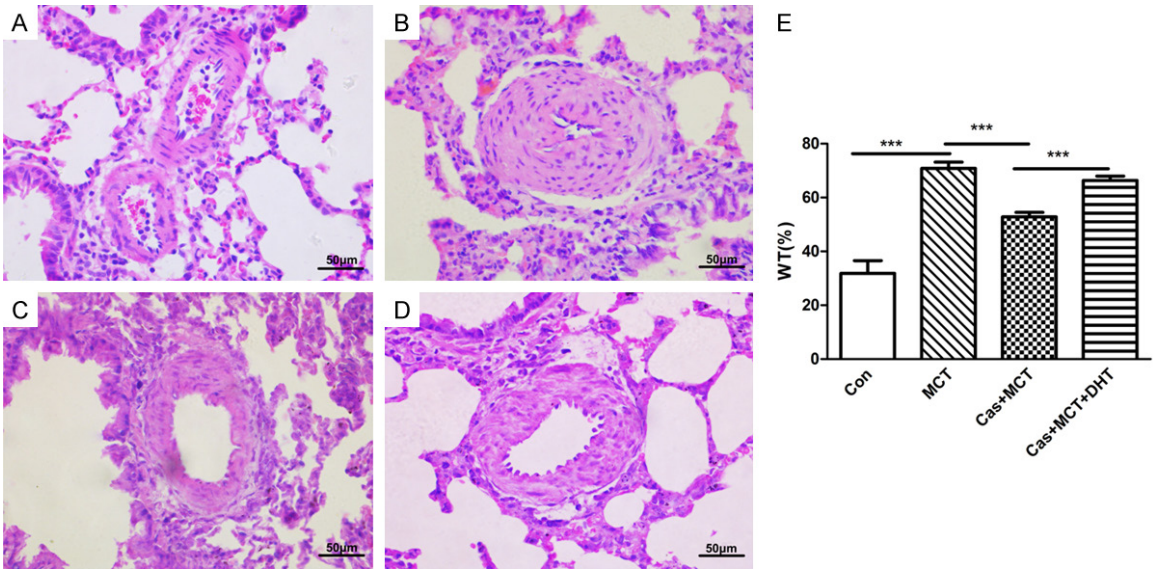

Figure 2. Effect of castration and/or DHT replacement on pulmonary remodeling in MCT-PH rats. (A-D) MCT-PH was induced in male SD rats as well as castrated rats with or without concomitant DHT repletion. After 3 weeks, WT of pulmonary artery was detected by HE staining. (E) Quantification of WT from (A-D). Note: (A) Con group; (B) MCT group; (C) Cas + MCT group; (D) Cas + MCT + DHT group; ***P<0.001 between groups. Magnification was ×400.

Castration improves myocardial hypertrophy and interstitial fibrosis in RV, which is reversed by DHT replacement

To further elucidate the effect of androgen on RVH in MCT-PH rats, we evaluated the effect of DHT on MCT-induced RV injury via the changes in cardiomyocyte size and fibrosis. As shown in **Figure 3A** and **3C**, HE staining showed hypertrophied and disordered cardiomyocytes in the RV of rats in MCT group compared with that in control group, and these maladaptive changes were restored by castration. However, the myocardial cross sectional area in Cas + MCT + DHT group was increased significantly compared with that in Cas + MCT group (P<0.001). Additionally, as shown in **Figure 3D** and **3E**, the mRNA expression levels of cardiac hypertrophic markers ANP and BNP in Cas + MCT + DHT group were significantly increased compared with that in Cas + MCT group. Subsequently, cardiac fibrosis was assessed, as shown in **Figure 3B** and **3F**, Sirius red staining in RV shows a significant increase in myocardial collagen volume fraction in MCT group compared with that in control group (P<0.001), in particular, castration in MCT-PH rats reduced collagen levels significantly compared with MCT group (P<0.001), which was aggrevated by DHT replacement (P<0.001). Transforming growth factor-β (TGF-β) plays an important role in the pathogenesis of cardiac fibrotic and hypertrophic remodeling. The expression of TGF-β was increased in the hypertrophied hearts induced by pressure overload [21, 22]. As shown in **Figure 3G**, the mRNA expression levels of TGF-β was increased in MCT group compared with that in control group (P<0.05). Castration in MCT-PH rats shows a decrease in TGF-β mRNA expression, which was reversed by DHT replacement (P<0.05). Interestingly, the DHT-induced increase of cardiomyocyte size and interstitial fibrosis in RV was even more serious than that in sham-castrated rats with MCT-PH (P<0.01 and P<0.001, respectively).

DHT induces proliferative and proapoptotic signaling in castrated rats with MCT-PH

Both of Ki67 and PCNA are the most widely used proliferating cell markers. To further evaluate the effect of DHT on pulmonary vascular proliferation, we observed Ki67 and PCNA expression in PA by immunofluorescence staining and western blotting, respectively. A significant increase of Ki67 positive cells (**Figure 4A-D**, **4H**) and the expression of PCNA (**Figure 4E** and **4I**) in the vascular walls was observed in MCT group in comparison to that in control group (P<0.001 and P<0.001, respectively), which was diminished by castration (P<0.05 and P<0.05, respectively). However, DHT (5

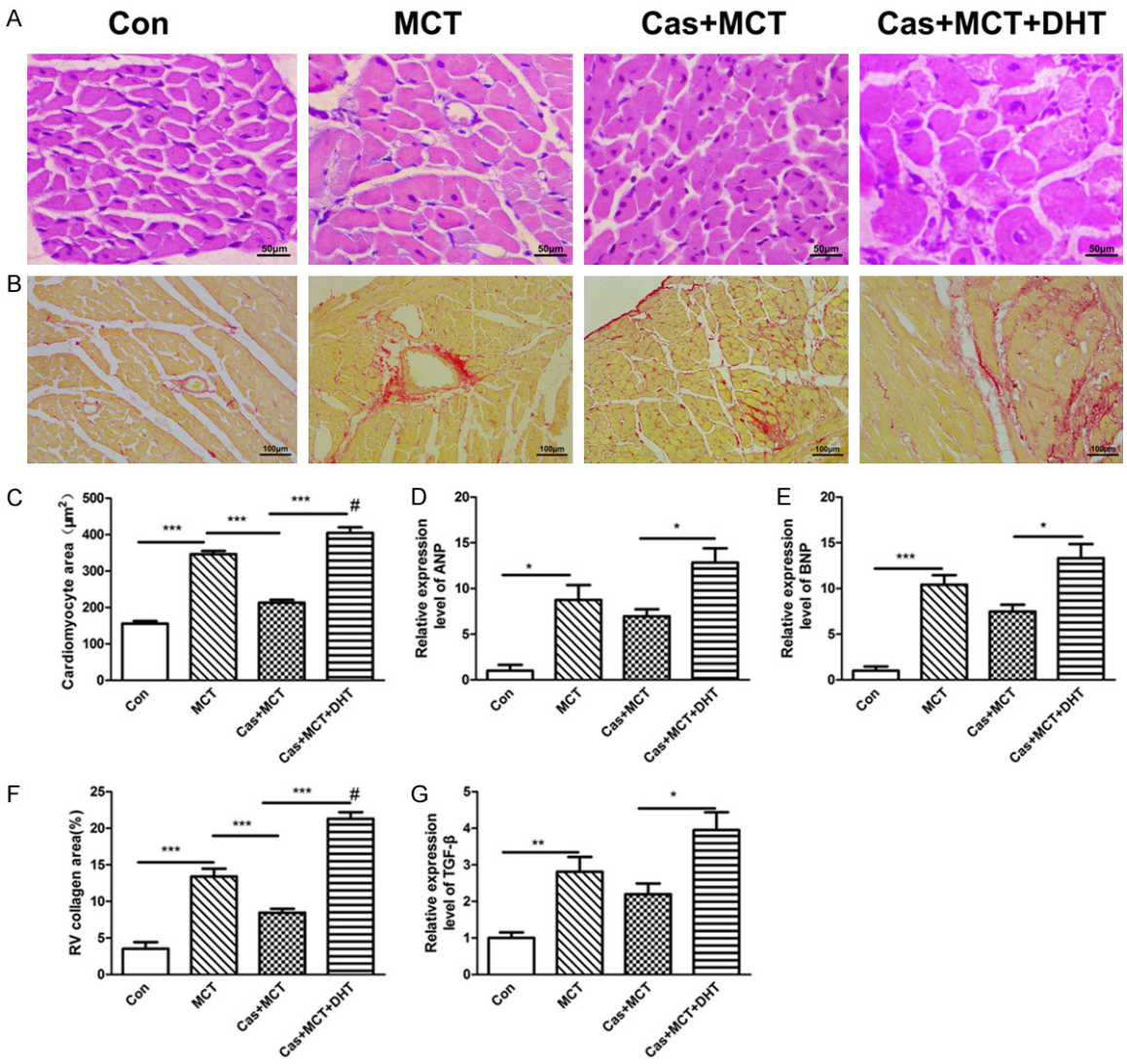

Figure 3. Effect of castration and/or DHT replacement on cardiac hypertrophy and fibrosis in MCT-PH rats. (A) Cross-sectional area of RV cardiomyocytes was detected by HE staining in rats. (B) The degree of RV collagen (red color) was analyzed by Sirius red staining. (C) Quantification of cross-sectional area of cardiomyocytes from (A). (D, E) The relative mRNA expression of ANP and BNP between groups. (F) Quantification of RV collagen area fraction from (B). (G) The relative mRNA expression of fibrosis markers (TGF-β) in RV. *P<0.05, **P<0.01, ***P<0.001 between groups. $^{\#}$P<0.01 vs. the MCT group. Magnification was ×400 (A) and ×200 (B).

mg/kg/d) significantly induced the expression of proliferating cells markers compared to that in castrated rats with MCT-PH (P<0.05).

In addition, the effect of DHT on apoptosis in rats with MCT-PH was examined by measuring the expression of apoptosis-associated proteins. As shown in **Figure 4F-K**, the level of Bax was increased significantly (P<0.001), while Bcl-2 was decreased in PA of MCT group (P<0.05), compared with that of control group, which was reversed by castration (P<0.05). In addition, DHT replacement in castrated rats with MCT-PH showed a trend of an opposite effect to castration.

DHT promotes the activity of pro-inflammatory cytokines and oxidative stress in castrated rats with MCT-PH

We examined inflammatory reaction in perivascular tissues. As shown in **Figure 5A**, a significant perivascular inflammatory cells infiltrated into lung tissue in the MCT group, and the overall inflammatory response was lessened relatively in Cas + MCT group, however, DHT aggra-

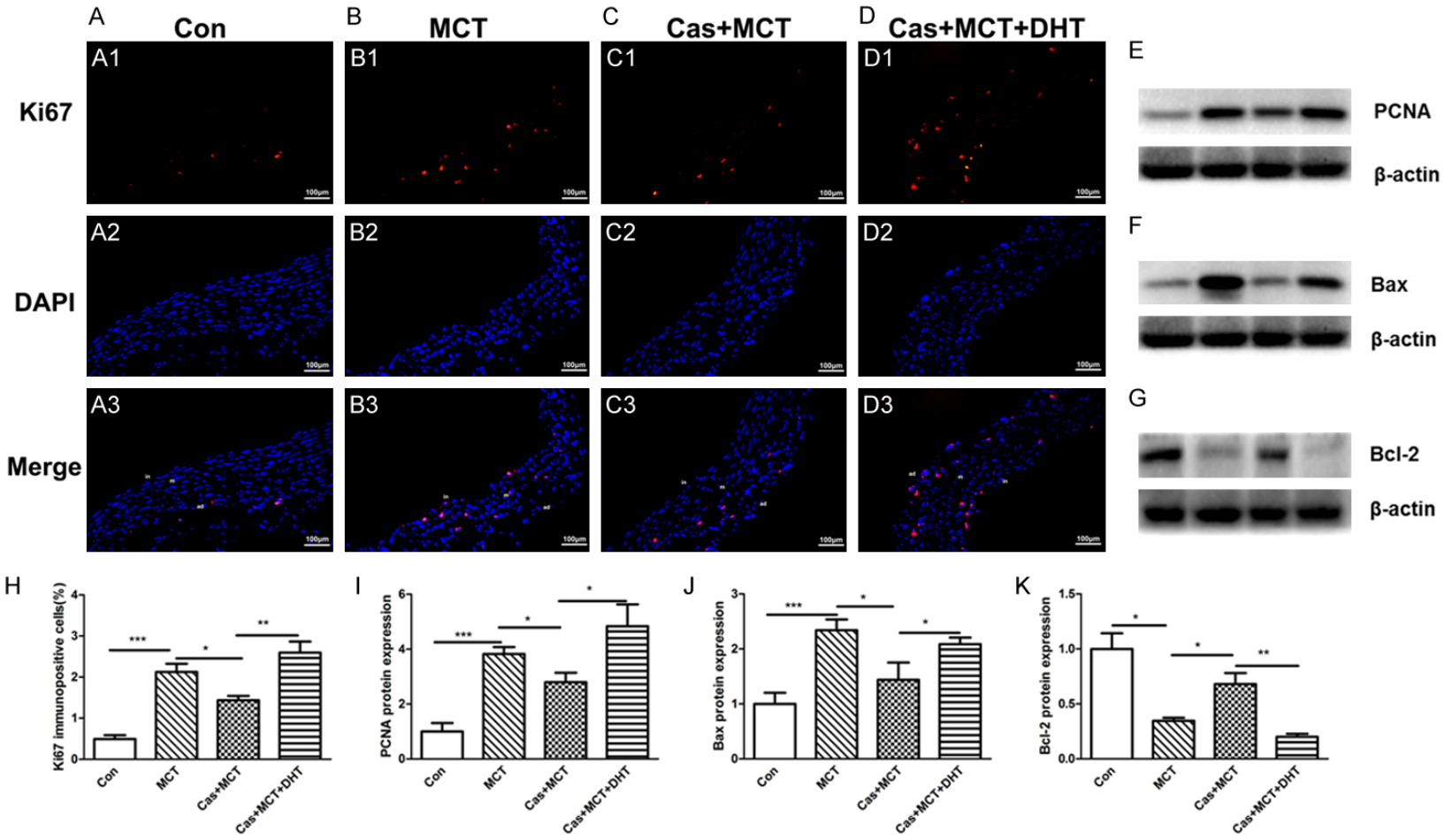

Figure 4. Effect of castration and/or DHT replacement on proliferation- and apoptosis-associated proteins in MCT-PH rats. Immunoblot analysis: (A-D, H) MCT-PH was induced in male SD rats as well as castrated rats with or without concomitant DHT repletion for 3 weeks. PA tissues were collected to evaluate Ki67 positive cells by immunofluorescence (red for Ki67 in (A1-D1), blue for nuclei in (A2-D2), purple for merge of Ki67 and nuclei in (A3-D3)). (E, I) The abundance of PCNA in PA was detected by WB. (F, G, J, K) The abundance of Bax and Bcl-2 in RV was detected by WB. Bar graphs are summary data. Note: in (intima), m (media); ad (adventia). $^{*}P<0.05$, $^{**}P<0.01$, $^{***}P<0.001$ between groups. Magnification = ×200.

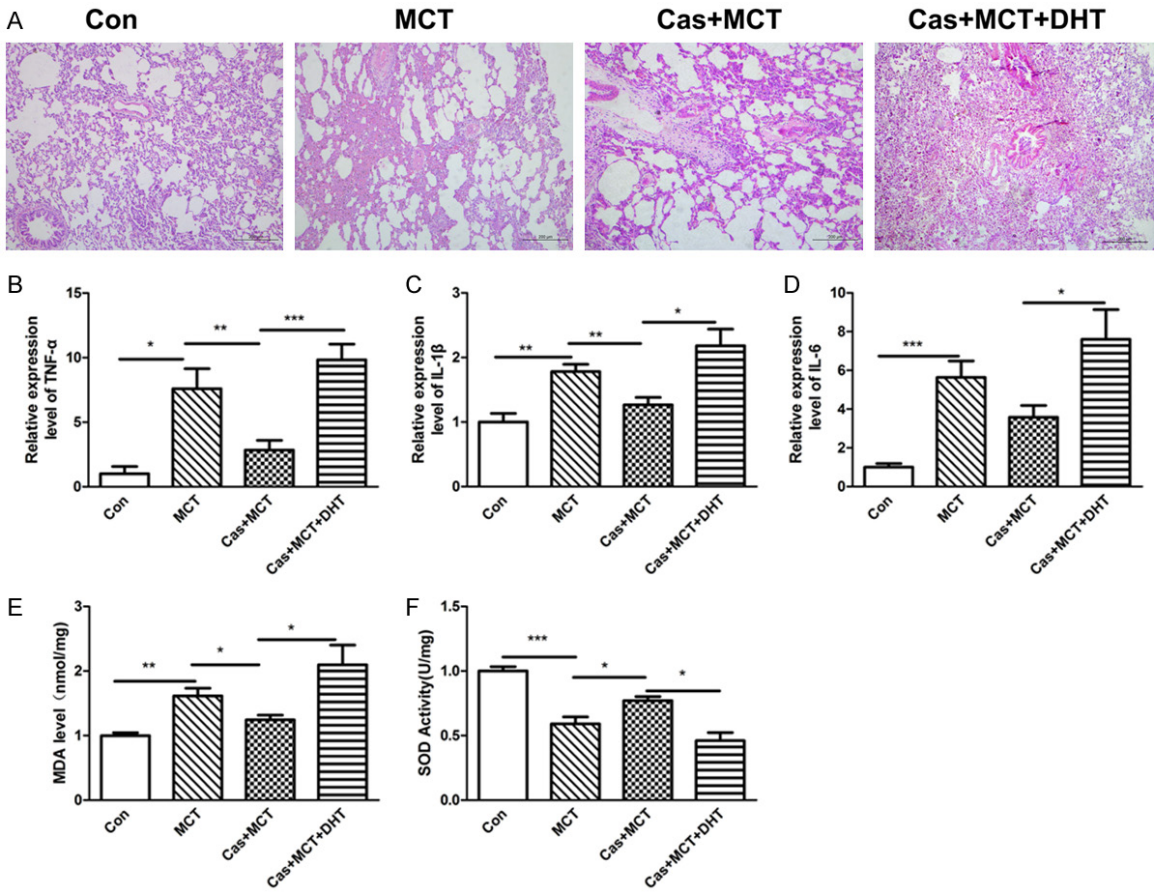

Figure 5. Effect of castration and/or DHT replacement on the inflammatory response and oxidative stress in MCT-PH rats. A. MCT-PH was induced in male SD rats as well as castrated rats with or without concomitant DHT repletion for 3 weeks. Inflammatory changes in perivascular tissues were evaluated by HE staining. B-D. The gene expression of inflammatory factors TNF-α, IL-1β and IL-6 in lung tissue was detected by real time PCR. E, F. The supernatant of lung tissue was collected to detect MDA content and SOD activity by ELISA. Bar graphs are summary data. *P<0.05, **P<0.01, ***P<0.001 between groups. Magnification = ×100.

vated the inflammation in castrated rats with MCT-PH. Real time PCR analysis showed that the expression of TNF-α, IL-6 and IL-1β mRNA was obviously up-regulated in MCT group compared with that in control group (**Figure 5B-D**, P<0.05), and castration down-regulated inflammatory response factors expression, which was reversed by DHT replacement (P<0.05).

We also evaluated the effect of DHT on PAH by detecting oxidative stress levels in MCT rats. As shown in **Figure 5E** and **5F**, the results showed that the MDA level was increased (P<0.01) and SOD activity was decreased markedly (P<0.001) in MCT group compared with the control group. Compared with MCT group, castration decreased the MDA level (P<0.05) and increased the activity of anti-oxidative SOD (P<0.05). Administration of DHT increased the MDA level (P<0.05) and inhibited SOD activity (P<0.05) in comparison to rats in Cas + MCT group, which indicated that DHT can aggravate oxidative stress.

DHT promotes matrix metalloproteinase-2 expression in castrated rats with MCT-PH

To further evaluate the effect of androgen on proteolytic degradation in PA, we detected MMP-2 expression in PA by immunofluorescence staining and western blotting, respectively. Compared with control group, MMP-2 positive cells (**Figure 6A-E**) and the protein level of MMP-2 (**Figure 6F** and **6G**) was elevated in the vascular walls in MCT group (P<0.001 and P<0.001, respectively), which was diminished by castration (P<0.001 and P<0.05, respectively). However, DHT (5 mg/kg/d) repla-

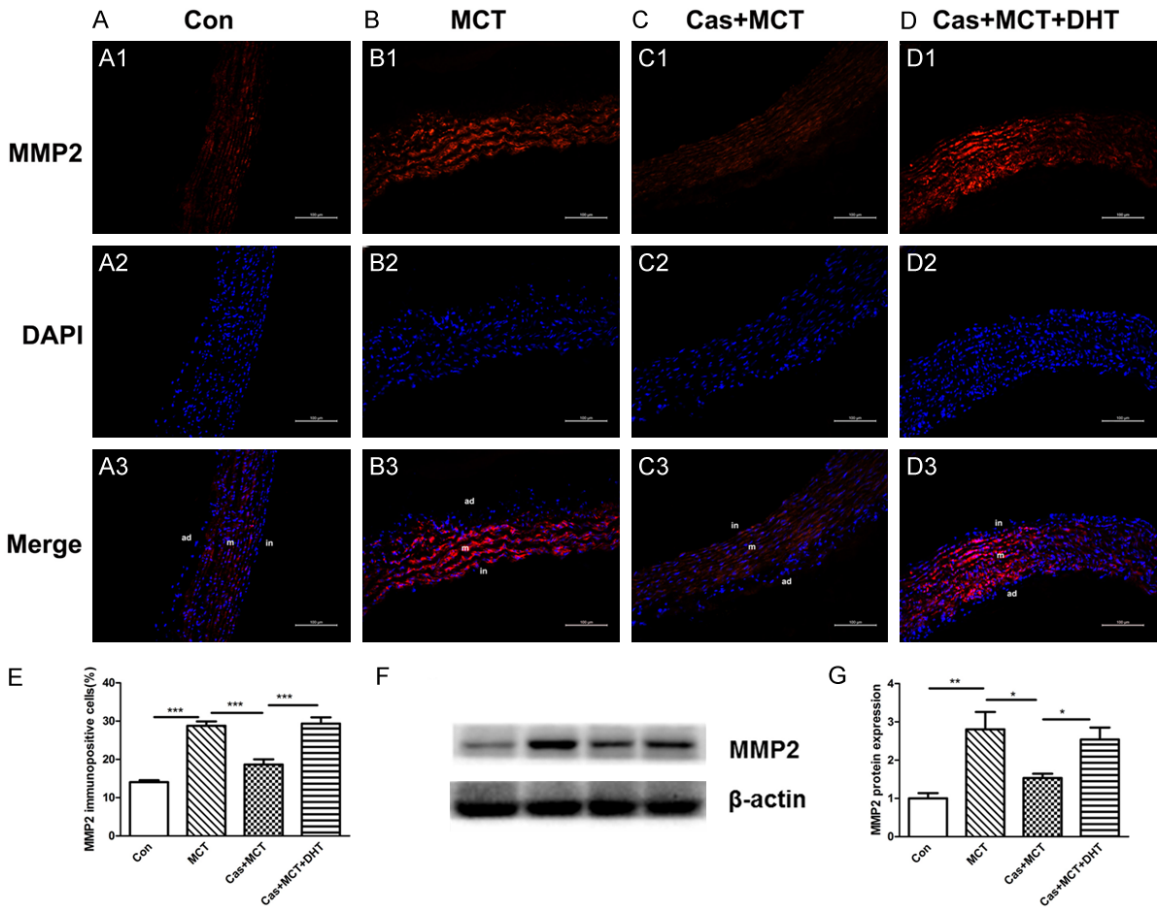

Figure 6. Effect of castration and/or DHT replacement on extracellular matrix metalloproteinase in MCT-PH rats. Immunoblot analysis: (A-E) MCT-PH was induced in male SD rats as well as castrated rats with or without concomitant DHT repletion for 3 weeks. PA tissues were collected to evaluate MMP2 positive cells by immunofluorescence (red for MMP-2 in (A1-D1), blue for nuclei in (A2-D2), pink for merge of MMP2 and nuclei in (A3-D3)). (F, G) The abundance of MMP2 in PA was detected by WB. Note: in (intima), m (media); ad (adventia). *P<0.05, ***P<0.001 between groups. Magnification = ×200.

cement significantly reversed this effect (P< 0.001 and P<0.05, respectively).

Discussion

We showed here that castration significantly reduced RVSP compared with the sham-castrated rats with MCT-PH, although it was still much higher than that in control rats. In contrast, DHT replacement significantly elevated RVSP compared to MCT-PH rats receiving castration, leading to a dramatic acceleration of estimated pulmonary pressure. These results demonstrated that castration significantly slowed the progression of PAH more impressively, DHT replacement accelerated RVSP to an even higher level than sham-castrated rats with MCT-PH. The effect of castration on hemodynamics is likely prevention rather than restoration, because RVSP in this model is significantly elevated at 3-wk time point [18].

Continuing elevated pulmonary vascular resistance can cause an increase in RV afterload and ultimately RV failure [23]. It is thought that in the early stage of PAH, the high pressure, pulmonary vascular resistance and stiffness are compensated by an adaptive “concentric” RV hypertrophy [24] to maintain cardiac output. However, with the low rate of cardiac cell regeneration and reduction in number of cardiomyocytes [25], cardiac fibrosis becomes the main repair process in the heart, which may cause “eccentric” remodeling in the latter stage. Castration prevented the adaptive features of RV remodeling, and DHT repletion (5 mg/kg/day) drastically promoted fibrosis, but in contrast, it only moderately restored the degree of

myocardial size. Therefore, we proposed that DHT may shift RVH into compensated eccentric remodeling. The result is consistent with other previous studies, in which T was proven to promote RV hypertrophic response to load stress [16], these observation are in accordance with current clinical data in which worse clinical outcomes in males with PAH than females [6, 26].

Aberrant vascular remodeling is considered to be a pathological hallmark of PAH, which is mainly manifested in the proliferation of PSMCs [27]. In our study, we observed a significant decrease in the vascular wall thickness and the expression of vascular proliferative markers such as Ki67 and PCNA in PA of castrated rats with MCT-PH compared to sham castration. These changes were partly prevented by daily administration of DHT (5 mg/kg), which indicated that DHT exerted deteriorated effect on the progression of PAH by promoting neointimal hyperplasia. We also observed increased expression of MMP-2 in PA tissue of MCT-PH rats. MMPs are involved in composition and remodeling of vascular wall. In response to angiogenic agents, endothelial-derived MMPs production in vivo and in vitro is increased to mediate proteolytic degradation of endothelial cell-cell interactions, which induce phenotype conversion in endothelial cells [28]. In addition, the correlation between MMP-2 and progression of PAH in PASMCs isolated both from idiopathic PAH patients and animal models indicated important roles in different vascular remodeling processes that involves smooth muscle cell proliferation, migration and intimal thickening [29, 30]. MMP-2 but not MMP-9 may contribute to this gelatinolytic activity since expression of MMP-9 was not observed in the PAH model. In our study, both endogenous androgen and exogenous DHT significantly upregulated MMP-2 expression in PA, which may partly explain its effect on neointimal hyperplasia.

Inflammation has been long recognized as an important pathogenetic element in PAH [31]. It was documented that perivascular inflammation correlated with parameters of pulmonary vascular remodeling and increased PAP in PAH [32], and inhibition of pulmonary inflammatory response can attenuate pulmonary vascular remodeling [33]. In addition, secreted cytokines may amplify inflammation and stimulate vascular remodeling, either directly or through the production of growth factors. It has been reported that cytokines such as TNF-α, IL-6 and IL-1β are elevated in MCT-PH and in the serum of PAH patients [31, 34]. In the present study, castration resulted in decreased inflammatory responses and pro-inflammation cytokines expression in the lung tissues in rats with MCT-PH. Furthermore, this anti-inflammation effect was reversed by DHT replacement. Thus, it seems that DHT may induce pulmonary vascular remodeling by upregulating the levels of inflammatory cytokines to increase the recruitment of perivascular inflammation.

Oxidative stress has been evidenced in the pathogenesis of cardiovascular disease such as heart failure, RVH and PAH [35, 36]. Increasing evidence suggests that oxidative stress leads to EC dysfunction and smooth muscle cell proliferation and hyperplasia eventually causing vascular remodeling. Our finding demonstrated that castration inhibited oxidative stress by decreasing MDA level and increasing SOD activity, and exogenous DHT exhibited an inducing effect on oxidative stress. In addition, EC apoptosis in the pulmonary vasculature might trigger pathological vascular remodeling and lead to severe PAH [37]. In the current study, we observed that MCT up-regulated the expression of pro-apoptotic markers, which is consistent with previous studies. However, castration attenuated MCT-induced pro-apoptotic effect, which was inhibited by DHT replacement, all these findings indicated that DHT may exert a detrimental effect on the progression of PAH by inducing oxidative stress and apoptosis.

In conclusion, we for the first time found the detrimental effects of androgen especially DHT on pulmonary arterial remodeling and RVH in a model of MCT-induced PAH by stimulating oxidative stress, inflammation, gelatinolytic activity, cell apoptosis and cell proliferation. Further research is required to better understand the role and mechanism of DHT in the pathophysiologic processes in vivo and their possible use as therapeutic targets.

Acknowledgements

This study was supported in part by the National Science Foundation of China (NSFC) Project (No. 81400357 and 81500184), and National

Science Foundation in Hunan Project (No. 2015JJ3145 and 2015SK20455).

Disclosure of conflict of interest

None.

Address correspondence to: Dr. Xiaohui Li, Department of Pharmacology, Xiangya School of Pharmaceutical Sciences, Central South University, Changsha 410013, Hunan, China. Tel: +8615874923132; E-mail: xiaohuili@csu.edu.cn; Dr. Weijun Cai, Department of Histology and Embryology, School of Basic Medicine, Central South University, Changsha 410013, Hunan, China. Tel: +8615874099375; E-mail: caiweijun@csu.edu.cn

References

[1] Docherty CK, Harvey KY, Mair KM, Griffin S, Denver N and MacLean MR. The role of sex in the pathophysiology of pulmonary hypertension. Adv Exp Med Biol 2018; 1065: 511-528.

[2] Zangiabadi A, De Pasquale CG and Sajkov D. Pulmonary hypertension and right heart dysfunction in chronic lung disease. Biomed Res Int 2014; 2014: 739674.

[3] Walker AM, Langleben D, Korelitz JJ, Rich S, Rubin LJ, Strom BL, Gonin R, Keast S, Badesch D, Barst RJ, Bourge RC, Channick R, Frost A, Gaine S, McGoon M, McLaughlin V, Murali S, Oudiz RJ, Robbins IM, Tapson V, Abenhaim L and Constantine G. Temporal trends and drug exposures in pulmonary hypertension: an American experience. Am Heart J 2006; 152: 521-526.

[4] Sitbon O, Benza RL, Badesch DB, Barst RJ, Elliott CG, Gressin V, Lemarie JC, Miller DP, Muros-Le Rouzic E, Simonneau G, Frost AE, Farber HW, Humbert M and McGoon MD. Validation of two predictive models for survival in pulmonary arterial hypertension. Eur Respir J 2015; 46: 152-164.

[5] Badesch DB, Raskob GE, Elliott CG, Krichman AM, Farber HW, Frost AE, Barst RJ, Benza RL, Liou TG, Turner M, Giles S, Feldkircher K, Miller DP and McGoon MD. Pulmonary arterial hypertension baseline characteristics from the REVEAL Registry. Chest 2010; 137: 376-387.

[6] Benza RL, Miller DP, Gomberg-Maitland M, Frantz RP, Foreman AJ, Coffey CS, Frost A, Barst RJ, Badesch DB, Elliott CG, Liou TG and McGoon MD. Predicting survival in pulmonary arterial hypertension: insights from the registry to evaluate early and long-term pulmonary arterial hypertension disease management (REVEAL). Circulation 2010; 122: 164-172.

[7] Jacobs W, van de Veerdonk MC, Trip P, de Man F, Heymans MW, Marcus JT, Kawut SM, Bogaard HJ, Boonstra A and Vonk Noordegraaf A. The right ventricle explains sex differences in survival in idiopathic pulmonary arterial hypertension. Chest 2014; 145: 1230-1236.

[8] Humbert M, Montani D, Perros F, Dorfmuller P, Adnot S and Eddahibi S. Endothelial cell dysfunction and cross talk between endothelium and smooth muscle cells in pulmonary arterial hypertension. Vascul Pharmacol 2008; 49: 113-118.

[9] Foderaro A and Ventetuolo CE. Pulmonary arterial hypertension and the sex hormone paradox. Curr Hypertens Rep 2016; 18: 84.

[10] Zhu YS. Molecular basis of steroid action in the prostate. Cellscience 2005; 1: 27-55.

[11] English KM, Jones RD, Jones TH, Morice AH and Channer KS. Gender differences in the vasomotor effects of different steroid hormones in rat pulmonary and coronary arteries. Horm Metab Res 2001; 33: 645-652.

[12] Rowell KO, Hall J, Pugh PJ, Jones TH, Channer KS and Jones RD. Testosterone acts as an efficacious vasodilator in isolated human pulmonary arteries and veins: evidence for a biphasic effect at physiological and supra-physiological concentrations. J Endocrinol Invest 2009; 32: 718-723.

[13] Dumas de La Roque E, Bellance N, Rossignol R, Begueret H, Billaud M, dos Santos P, Ducret T, Marthan R, Dahan D, Ramos-Barbon D, Amor-Carro O, Savineau JP and Fayon M. Dehydroepiandrosterone reverses chronic hypoxia/reoxygenation-induced right ventricular dysfunction in rats. Eur Respir J 2012; 40: 1420-1429.

[14] Dumas de la Roque E, Savineau JP and Bonnet S. Dehydroepiandrosterone: a new treatment for vascular remodeling diseases including pulmonary arterial hypertension. Pharmacol Ther 2010; 126: 186-199.

[15] Alzoubi A, Toba M, Abe K, O'Neill KD, Rocic P, Fagan KA, McMurtry IF and Oka M. Dehydroepiandrosterone restores right ventricular structure and function in rats with severe pulmonary arterial hypertension. Am J Physiol Heart Circ Physiol 2013; 304: H1708-1718.

[16] Hemnes AR, Maynard KB, Champion HC, Gleaves L, Penner N, West J and Newman JH. Testosterone negatively regulates right ventricular load stress responses in mice. Pulm Circ 2012; 2: 352-358.

[17] Wen J, Zhao Y, Li J, Weng C, Cai J, Yang K, Yuan H, Imperato-McGinley J and Zhu YS. Suppression of DHT-induced paracrine stimulation of endothelial cell growth by estrogens via prostate cancer cells. Prostate 2013; 73: 1069-1081.

[18] Yang DL, Zhang HG, Xu YL, Gao YH, Yang XJ, Hao XQ and Li XH. Resveratrol inhibits right

ventricular hypertrophy induced by monocrotaline in rats. Clin Exp Pharmacol Physiol 2010; 37: 150-155.
[19] Pluchino N, Ninni F, Casarosa E, Giannini A, Merlini S, Cubeddu A, Luisi M, Cela V and Genazzani AR. Sex differences in brain and plasma beta-endorphin content following testosterone, dihydrotestosterone and estradiol administration to gonadectomized rats. Neuroendocrinology 2009; 89: 411-423.
[20] Weng C, Cai J, Wen J, Yuan H, Yang K, Imperato-McGinley J and Zhu YS. Differential effects of estrogen receptor ligands on regulation of dihydrotestosterone-induced cell proliferation in endothelial and prostate cancer cells. Int J Oncol 2013; 42: 327-337.
[21] Dobaczewski M, Chen W and Frangogiannis NG. Transforming growth factor (TGF)-beta signaling in cardiac remodeling. J Mol Cell Cardiol 2011; 51: 600-606.
[22] Ma ZG, Yuan YP, Zhang X, Xu SC, Wang SS and Tang QZ. Piperine attenuates pathological cardiac fibrosis via PPAR-gamma/AKT pathways. EBioMedicine 2017; 18: 179-187.
[23] Badagliacca R, Poscia R, Pezzuto B, Papa S, Reali M, Pesce F, Manzi G, Gianfrilli D, Ciciarello F, Sciomer S, Biondi-Zoccai G, Torre R, Fedele F and Vizza CD. Prognostic relevance of right heart reverse remodeling in idiopathic pulmonary arterial hypertension. J Heart Lung Transplant 2017; [Epub ahead of print].
[24] Handoko ML, de Man FS, Allaart CP, Paulus WJ, Westerhof N and Vonk-Noordegraaf A. Perspectives on novel therapeutic strategies for right heart failure in pulmonary arterial hypertension: lessons from the left heart. Eur Respir Rev 2010; 19: 72-82.
[25] Vicinanza C, Aquila I, Scalise M, Cristiano F, Marino F, Cianflone E, Mancuso T, Marotta P, Sacco W, Lewis FC, Couch L, Shone V, Gritti G, Torella A, Smith AJ, Terracciano CM, Britti D, Veltri P, Indolfi C, Nadal-Ginard B, Ellison-Hughes GM and Torella D. Adult cardiac stem cells are multipotent and robustly myogenic: c-kit expression is necessary but not sufficient for their identification. Cell Death Differ 2017; 24: 2101-2116.
[26] Humbert M, Sitbon O, Yaici A, Montani D, O'Callaghan DS, Jais X, Parent F, Savale L, Natali D, Gunther S, Chaouat A, Chabot F, Cordier JF, Habib G, Gressin V, Jing ZC, Souza R, Simonneau G; French Pulmonary Arterial Hypertension Network. Survival in incident and prevalent cohorts of patients with pulmonary arterial hypertension. Eur Respir J 2010; 36: 549-555.
[27] Guignabert C, Tu L, Le Hiress M, Ricard N, Sattler C, Seferian A, Huertas A, Humbert M and Montani D. Pathogenesis of pulmonary arterial hypertension: lessons from cancer. Eur Respir Rev 2013; 22: 543-551.
[28] van Hinsbergh VW, Koolwijk P. Endothelial sprouting and angiogenesis: matrix metalloproteinases in the lead. Cardiovasc Res 2008; 78: 203-212.
[29] Lepetit H, Eddahibi S, Fadel E, Frisdal E, Munaut C, Noel A, Humbert M, Adnot S, D'Ortho MP, Lafuma C. Smooth muscle cell matrix metalloproteinases in idiopathic pulmonary arterial hypertension. Eur Respir J 2005; 25: 834-842.
[30] Frisdal E, Gest V, Vieillard-Baron A, Levame M, Lepetit H, Eddahibi S, Lafuma C, Harf A, Adnot S, Dortho MP. Gelatinase expression in pulmonary arteries during experimental pulmonary hypertension. Eur Respir J 2001; 18: 838-845.
[31] Rabinovitch M, Guignabert C, Humbert M and Nicolls MR. Inflammation and immunity in the pathogenesis of pulmonary arterial hypertension. Circ Res 2014; 115: 165-175.
[32] Stacher E, Graham BB, Hunt JM, Gandjeva A, Groshong SD, McLaughlin VV, Jessup M, Grizzle WE, Aldred MA, Cool CD and Tuder RM. Modern age pathology of pulmonary arterial hypertension. Am J Respir Crit Care Med 2012; 186: 261-272.
[33] Luan Y, Chao S, Ju ZY, Wang J, Xue X, Qi TG, Cheng GH and Kong F. Therapeutic effects of baicalin on monocrotaline-induced pulmonary arterial hypertension by inhibiting inflammatory response. Int Immunopharmacol 2015; 26: 188-193.
[34] Groth A, Vrugt B, Brock M, Speich R, Ulrich S and Huber LC. Inflammatory cytokines in pulmonary hypertension. Respir Res 2014; 15: 47.
[35] Hansen T, Galougahi KK, Celermajer D, Rasko N, Tang O, Bubb KJ and Figtree G. Oxidative and nitrosative signalling in pulmonary arterial hypertension - implications for development of novel therapies. Pharmacol Ther 2016; 165: 50-62.
[36] Siti HN, Kamisah Y and Kamsiah J. The role of oxidative stress, antioxidants and vascular inflammation in cardiovascular disease (a review). Vascul Pharmacol 2015; 71: 40-56.
[37] Taraseviciene-Stewart L, Kasahara Y, Alger L, Hirth P, Mc Mahon G, Waltenberger J, Voelkel NF and Tuder RM. Inhibition of the VEGF receptor 2 combined with chronic hypoxia causes cell death-dependent pulmonary endothelial cell proliferation and severe pulmonary hypertension. FASEB J 2001; 15: 427-438.